Anomalous Behavior of Thermosetting Systems After Cure vs. Chemical Conversion: A Normalized Conversion–Temperature–Property Diagram

R. A. VENDITTI* and J. K. GILLHAM†

Polymer Materials Program, Department of Chemical Engineering, Princeton University, Princeton, New Jersey 08544

SYNOPSIS

Isothermal properties of thermosetting materials after cure, such as density and modulus, pass through maximum and minimum values with increasing chemical conversion. In this report observed decreases in modulus and density at isothermal temperatures below the glass-transition temperature, T_g, are termed "anomalous." Four diepoxide (diglycidyl ether of bisphenol A) and tetrafunctional diamine (trimethylene glycol di-*p*-aminobenzoate) high T_g thermosetting systems with different ratios of amine to epoxy were investigated for the purpose of analyzing the evolution of the isothermal properties with increasing conversion. The density, T_g, and modulus of the materials with increasing conversion were measured by a combination of dilatometric, differential scanning calorimetry, and torsional braid analysis techniques. The results are presented in the form of conversion–temperature–property (T_gTP) diagrams with modulus and density as the properties. T_g is used as a direct measure of conversion based on the one-to-one relationship between T_g and conversion. The property-conversion behavior of the systems with different ratios of amine to epoxy show similar behavior if T_g is used as the measure of conversion and the data are normalized with respect to T_g at a conversion corresponding to the lower limit of the conversion range at which a maximum in the isothermal modulus occurs. The conversion corresponding to molecular gelation, ${}_{gel}T_g$, correlates with the lower limit of the conversion range at which the maximum in isothermal modulus occurs; ${}_{gel}T_g$ also marks a change in the behavior of the sub-T_g mechanical relaxations vs. conversion. The conversion corresponding to the maximum in isothermal modulus vs. conversion correlates with the conversion corresponding to the maximum in isothermal density vs. conversion.

INTRODUCTION

There is evidence in the literature pertaining to the so-called "anomalous behavior" of the isothermal density in the glassy state of thermosetting materials decreasing with increasing chemical conversion (or increasing glass-transition temperature, T_g).[1–6] The changes in density with conversion have been correlated with other properties of thermosets. For high T_g epoxy-amine systems, the changes in density at 25°C[1] have been correlated with other properties at 25°C such as the modulus passing through a maximum with increasing conversion[7,8] and the equilibrium moisture content increasing at later stages of conversion.[9] Other researchers also found changes in isothermal properties, such as high strain strength,[10] equilibrium moisture absorption,[2] initial water diffusion coefficient,[2] and low-strain modulus,[11,12] to reflect the anomalous change in density with conversion.

Noncrosslinking thermosetting systems that harden due to reactions during cure, for example, a linear polyamic acid ester to polyimide system, also show anomalous behavior of the isothermal modulus decreasing with increasing conversion.[13]

* Present address: Department of Wood and Paper Science, Box 8005, North Carolina State University, Raleigh, NC, 27695-8005.

† To whom correspondence should be addressed

Journal of Applied Polymer Science, Vol. 56, 1687–1705 (1995)
 CCC 0021-8995/95/131687-19

It is not possible to fully understand the glassy state behavior of thermosetting materials without understanding the anomalous behavior. It is important therefore to identify the sources that can contribute to the changing density in the glassy state of a material after cure vs. chemical conversion. Figure 1 is a flow sheet of some of the phenomena that determine the glassy state density of a single phase thermosetting system and examples of processes and properties that are intimately related to the density. Analysis of the anomalous behavior is complicated by the multitude of interrelated variables that have an effect on the density. These include temperature gradients during solidification (i.e., vitrification), constraints due to adhesion to a substrate or an enclosure, and other processing variables. Use of solvents and catalysts (more generally, any small molecule) that may plasticize the polymer must be considered when investigating density trends. Molding techniques can have an effect on the density of the material (e.g., frozen-in flow patterns can result in anisotropic behavior of the solid). Thermal degradation reactions that occur at high cure temperatures, T_{cure}, which are utilized in an attempt to induce "full" conversion, should also be considered.

The anomaly has been analyzed by measuring other properties that depend on density. However, because these properties are not a function of density alone, caution must be made in relating the anomalous density behavior to them. Water absorption is an example of a property that may change during cure in epoxy systems due to both density changes and changes in the polarity of the internal structure (e.g., concentration of hydroxyl groups in an epoxy-

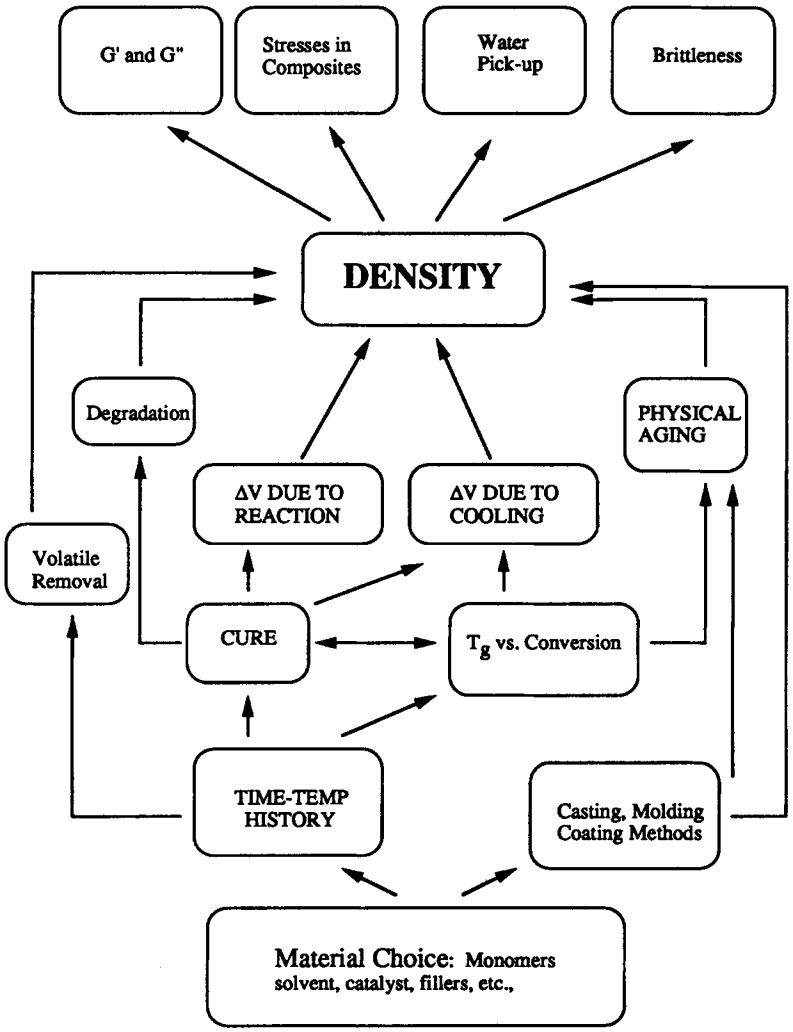

Figure 1 Schematic diagram showing some of the factors and processes (bottom) that affect the density of a thermosetting system and examples of properties (top) that depend on density.

amine reacting system). The modulus of a thermosetting system is affected by density and also by other quantities, such as intermolecular forces, intramolecular forces, molecular structure (e.g., crosslink concentration and molecular weight), temperature, and relaxational events.

Physical aging, the spontaneous process of a nonequilibrium glassy material to densify in an attempt to attain its equilibrium state, plays a role in changing the glassy state properties.[1,14–19] Physical aging alters the free volume, the macroscopic volume, the modulus, etc., of a glass. Physical aging effects arise during cure (when T_g rises above T_{cure}), during storage below T_g, and from different cooling rates from above T_g into the glassy state. It is necessary to identify physical aging effects when investigating the behavior of thermosets vs. conversion.

Two approaches can be used to alter the concentration of crosslinking sites in thermosetting systems. One is to vary the ratio of the different monomers in the initial formulation so that after full thermal cure the systems have different crosslink concentrations. Complications arise due to the uncertainty of the different systems to achieve full conversion (i.e., complete conversion of the deficient species). Small concentrations of unreacted material in a thermosetting system can have a significant influence on material behavior; for example, T_g may increase dramatically when the chemical conversion of a thermosetting system approaches completion.[20]

Another approach involves using a single initial reactive thermosetting formulation and comparing its properties vs. chemical conversion from the uncured state (no crosslinks) to the fully cured state (maximum crosslinks). This approach is particularly attractive if conversion uniquely relates to molecular structure. The molecular architecture can be inferred at any conversion for different time and temperature paths of reaction if the kinetics of the competing reactions are known. This method has the advantage that it is not necessary to attempt full conversion of different formulations for comparison. Complications arise due to the handling and characterizing of undercured specimens. Ungelled specimens tend to be brittle below their T_g, and flow above their T_g. Also, undercured specimens may react during characterization at temperatures above or near the previous cure temperature (e.g., during measurement of T_g). It is noted that for both approaches to changing the internal structure, the structures being compared differ more than in crosslinking density.

This report describes use of the above two approaches to investigate the changes of properties with increase of conversion. Measurements of properties (i.e., modulus and density) of a diglycidyl ether of bisphenol A (diepoxide, DGEBA) and a trimethylene glycol di-*p*-aminobenzoate (tetrafunctional aromatic diamine, TMAB) high T_g thermosetting system with different ratios of amino hydrogen atoms to epoxide groups (r) vs. conversion are presented. Precautions have been taken to compare specimens in which the effects of physical aging have been minimized. T_g is used as a direct measure of conversion on the basis of experimental results showing a one-to-one relationship between T_g and conversion.[20–23]

The chemical kinetics of this thermosetting family[20–22,24] and the effect of physical aging on the dynamic mechanical behavior of the material with $r = 1$ in the fully cured state[17] and vs. chemical conversion[19] have been reported.

The isothermal behavior of properties measured after thermal cure vs. chemical conversion may be succinctly summarized and related to events such as gelation, vitrification, and other transitions by using a plot with conversion, as measured by T_g, and temperature as coordinates for a base plane and projecting the values of a physical property onto the base plane. The resulting plot is termed a conversion–temperature–property (T_gTP) diagram.[7,8,12,13] It is shown herein that the T_gTP diagrams constructed using the low-strain shear modulus and the density as the property are qualitatively the same for measurement temperatures above the T_g of the unreacted formulation, T_{g0}.

An integrated review of research in our laboratory on the cure and evolution of properties of thermosetting systems has been published.[25] The present work forms part of a Ph.D. thesis.[26]

EXPERIMENTAL

Chemical Systems

The systems investigated were formulated with four different ratios of a diglycidyl ether of bisphenol A (DGEBA) [DER332, Dow Chemical Co.] and the tetrafunctional aromatic diamine, trimethylene glycol di-p-aminobenzoate (TMAB) [Polacure 740M, Air Products Co.]. The chemical structures and principal reactions are shown in Figure 2. The epoxy monomer is a viscous liquid at 25°C and has a theoretical epoxide equivalent weight, EEW, of 174.4 g/eq (determined by bromine titration by Dow Chemical Co., cf. EEW = 170 g/eq for the pure chemical). The amine curing agent is a highly crystalline solid

THERMOSETTING SYSTEM: REACTANTS

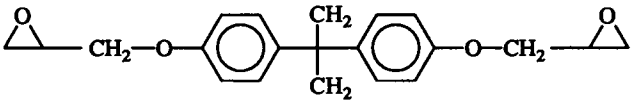

diglycidyl ether of bisphenol-A (DGEBA)

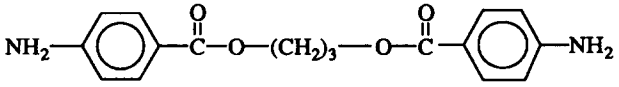

trimethylene glycol di-p-aminobenzoate (TMAB)

REACTIONS:

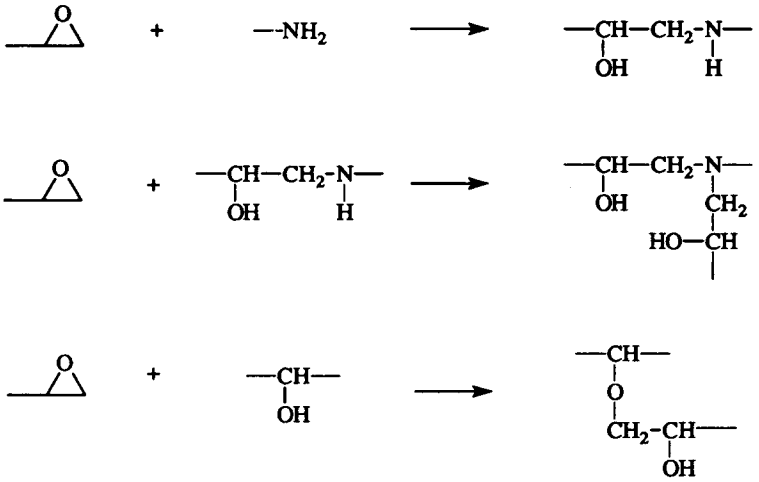

Figure 2 Chemical reactants and reactions.

at room temperature (mp = 125°C) with a theoretical amino hydrogen equivalent weight of 78.5 g/eq. The principal parameters of the uncured and fully cured systems are defined and included in Table I.

During thermal cure, at all ratios of amine to epoxy, the epoxy groups react with primary and secondary amino hydrogens (Fig. 2). In epoxy-rich systems, the excess epoxy groups may react with hydroxyl groups that form by the epoxy/amine reaction. The reaction of epoxy with hydroxyl in the epoxy-rich systems generally occurs after the more reactive amine groups have been depleted.[22]

Mixing Procedure

Four different mixtures, with ratios (r) of amino hydrogen atoms to epoxide groups, r = 1.2, 1.0, 0.9, and 0.8, were prepared according to the following procedure. The crystalline amine was added to the heated liquid epoxy monomer at 100°C. The mixture, approximately 50 g, was then vigorously stirred for 30 min. This procedure was adopted to ensure homogenous mixing and to avoid the use of solvent, the presence of which could complicate the chemical kinetics and the determination of the chemical

Table I Principal Parameters for DGEBA/TMAB Systems

r (1)	X_{gel} (2)	T_{g0} (3)	$T_{\gamma 0}$ (4)	${}_eT_g$ (min) (5)	${}_{gel}T_g$ (6)	$T_{g\infty}$ (7)	$T_{\beta\infty}$ (8)
∞		23	−124				
1.2	0.53	11	−156	39	47	164	−39
1.0	0.58	−1	−155	36	42	180	−44
0.9	0.61	−1	−156	44		178	−44
0.8	0.65	−6	−156	50	57	188	−52
0		−14	−149				

(1) r is the ratio of amino hydrogens to epoxide groups in the initial formulation. $r = \infty$ corresponds to pure TMAB and $r = 0$ corresponds to pure DER 332.

(2) X_{gel} is the molecular gelation conversion from Flory's theory.[30,31]

(3) T_g of the unreacted system.

(4) Glassy-state relaxation temperature of the unreacted system.

(5) ${}_eT_g$(min) is the minimum value of ${}_eT_g$. ${}_eT_g$ is the T_g at a conversion corresponding to a maximum in isothermal modulus vs. conversion (see text).

(6) ${}_{gel}T_g$ is the value of T_g at a conversion corresponding to molecular gelation. Values of ${}_{gel}T_g$ were obtained from T_g vs. conversion data in Gillham et al.[20-22] Values of T_g vs. conversion in Gillham et al.[20-22] were acquired using differential scanning calorimetry.

(7) T_g of the fully cured system.

(8) Glassy-state relaxation temperature of the fully reacted system.

structure vs. properties behavior of the material.[20] Immediately after mixing, the liquid was degassed under vacuum ($\cong$ 1 torr) at 75°C for 15 min. The resulting clear viscous liquid mixture was poured into numerous aluminum weighing pans, which were individually sealed in plastic bags, kept inside a dessicator, and stored in the freezer part of a refrigerator ($T = -20$°C, i.e., below the T_g of the unreacted material).

Torsional Braid Analysis (TBA)

TBA, which uses a composite specimen as the active part of a freely oscillating torsional pendulum, was performed on the four samples with different ratios of amino hydrogen to epoxide. Each sample was taken out of the freezer and allowed to stand at 25°C for 30 min inside the dessicator before removal. A heat-cleaned-in-air glass braid was dipped in the viscous reactive liquid mixture at room temperature for 30 min. The impregnated glass braid was then squeezed between aluminum foil to remove excess liquid material and to insure good wetting of the glass filaments. The final amount of material on the braid was approximately 15 mg. The specimen (dimensions approximately 1 mm in diameter and 50 mm in length) was mounted to form the TBA inner pendulum, which was inserted into the preheated chamber of the TBA instrument (40°C). All experiments were performed in an atmosphere of flowing helium. Reviews of the TBA technique have been published.[25,27,28] The automated instrument is available from Plastics Analysis Instruments, Inc. (Princeton, NJ).

In the TBA experiment, the torsion pendulum is intermittently set into motion to produce a series of freely damped waves. The frequency and logarithmic decrement of the free oscillations in each wave are determined; they are related to the in-phase shear modulus and tan δ of the composite specimen. The reported parameters of the TBA experiment are the relative rigidity (f^2), logarithmic decrement ($\Delta \approx \pi \tan \delta$), and relative out-of-phase shear modulus (aG''), as defined[27]:

$$f^2 \cong \frac{G'}{KI(2\pi)^2} \tag{1}$$

$$\Delta = \ln\left(\frac{A_i}{A_{i+1}}\right) \cong \pi \frac{G''}{G'} = \pi \tan \delta \tag{2}$$

$$aG'' \equiv f^2\Delta \cong \frac{\pi G''}{KI(2\pi)^2} \tag{3}$$

where f is the frequency of oscillation, G' is the in-phase shear modulus, G'' is the out-of-phase shear modulus, K is a geometric constant for a given specimen, I is the moment of rotational inertia of the moving parts of the pendulum, A_i and A_{i+1} are the amplitudes of successive peaks in the damped wave, and δ is the phase angle between stress and strain. The constant $a = \pi/KI(2\pi)^2$ is shown in eq. (3). The relative rigidity is proportional to the in-phase shear modulus and is therefore referred to as the modulus in this work. The frequency typically ranges from 0.2 to 3 Hz; measurements of frequency are sensitive to changes of 0.0001 Hz. T_g occurs at about 0.7 Hz; T_β and T_γ (both less than T_g) occur at about 1.1 Hz for

all specimens. All heating and cooling rates used in the TBA experiments were 1°C/min and 1.5°C/min, respectively. TBA measurements were taken at approximately 2°C intervals during temperature ramps.

Descriptions of the curing and measuring procedures in the TBA experiment follow. An uncured specimen was initially heated from 40 to 100°C before being cooled to −180°C. Dynamic mechanical measurements obtained during cooling (and heating) provided the modulus (relative rigidity) and the mechanical damping (logarithmic decrement and relative loss modulus) data vs. temperature. The temperatures of the maxima in the relative loss modulus obtained on cooling were used to assign the values of the relaxation temperatures, i.e., the glass-transition (relaxation) temperature (T_g) and the sub-T_g glassy state relaxation temperatures (T_β and T_γ, where $T_\beta > T_\gamma$). Data on cooling (rather than on heating) were utilized to minimize the effect of physical aging on the properties of the material. The specimen was then heated to above its T_g where additional reaction could occur and raise the value of T_g. The specimen was then cooled to −180°C while the dynamic mechanical behavior was obtained. The heating and cooling cycle was performed approximately 15 more times with progressively higher maximum temperatures until measurements had been taken on the specimen from the uncured to the fully cured state. This involved heating eventually to above $T_{g\infty}$, the highest measured value of T_g, for the four specimens. A single TBA specimen was used for each of the four systems.

Data for the isothermal modulus vs. conversion are reported using data obtained during cooling. The corresponding data for isothermal mechanical loss (Δ and aG'') are not reported here. It is assumed that the specimen had a constant mass and unchanged dimensions throughout the experiment. It is also assumed that microcracking was negligible for the temperature-conversion range of the data reported. An absence of hysteresis in the modulus vs. temperature plots between cooling and subsequent heating at a given conversion is evidence for the absence of microcracking.

The TBA unit is a convenient oven for heating and cooling small specimens at controlled rates in an inert atmosphere (without performing torsional pendulum experiments). A holding cell, designed for the TBA unit, allows 12 specimens, each with dimensions less than $10 \times 10 \times 4$ mm, to be supported within the TBA oven. Specimens that were to be analyzed in a density gradient column or by a differential scanning calorimeter were thermally treated in an atmosphere of flowing helium in the TBA oven prior to analysis (see following).

Preparation and Curing Procedure of Specimens for Dilatometric and Differential Scanning Calorimetric (DSC) Experiments

The system with $r = 1.0$ was used for density and thermal expansion coefficient measurements and for DSC experiments. The following procedure was performed repeatedly to produce specimens with different extents of cure. The initial reactive mixture, inside its plastic bag, was removed from the freezer and allowed at least 20 min to reach room temperature before being taken out of the bag (in order to prevent condensation of moisture from the atmosphere on the surface of the cold material). A portion of the liquid mixture was poured into an aluminum dish and degassed in a vacuum oven for 15 min at 75°C ($\cong$ 1 torr). The degassed liquid mixture was used to fill a heated multicavity aluminum mold (50°C) that was lined with aluminum foil. The mold contained cavities that resulted in disk-shaped specimens for density gradient column measurements (with diameter approximately 5 mm, thickness approximately 1 mm, mass approximately 25 mg). A portion of the degassed liquid mixture was also used to fill aluminum molds lined with aluminum foil that produced specimens with a rectangular shape (width approximately 6 mm, length approximately 7 cm, thickness approximately 0.6 mm) for measurements of thermal expansion coefficients. Portions of the degassed liquid mixture were also placed into six DSC pans that were then sealed under nitrogen (mass of sample per pan $\sim$ 10 mg) for subsequent DSC experiments.

Specimens of the three types were then placed together inside a large, temperature programmable oven at ambient temperature and pressure. The oven was purged continuously with nitrogen. The temperature was then raised at 5°C/min to a predetermined cure temperature, T_{cure}, held isothermally at the cure temperature for 2 h, and then cooled at 5°C/min to 40°C (see below). The partially and fully cured specimens were then removed from the oven.

At this juncture the values of T_g of the specimens were determined (see later) using two of the DSC specimens; these two DSC specimens were not used for any subsequent experiments. The values of T_g were used to determine the maximum temperature for further thermal treatment, as is described in the next paragraph. The rectangular specimens for thermal expansion coefficient measurements were peeled from the aluminum foil and stored inside a

dessicator for analysis at a later time. The density gradient column specimens, or simply "disks," were removed from the aluminum foil. The disks were inspected using a polarizing light microscope. All disk specimens used for further study were free from visible voids, bubbles, and cracks that could affect the measured macroscopic density of the material.

For each cure condition (i.e., as defined by the maximum temperature of cure), the disks (removed from the aluminum mold and foil) and the remaining DSC specimens were then heated in the TBA oven at 5°C/min to 20°C above their DSC-determined T_g values, held at this temperature for 20 min, and then cooled at a controlled rate of 5°C/min to 25°C. This thermal treatment was performed in the TBA oven so that the specimens could be cooled at a constant rate of 5°C/min to 25°C (the other larger oven was capable of cooling at a constant rate of 5°C only to 40°C). This additional thermal treatment was also intended to remove physical aging effects that may have arisen during cure and to relieve stresses that may have built up between the specimen and the aluminum foil. The disks were again inspected using a polarizing light microscope. The disks for density determinations and the DSC specimens were analyzed within an hour of the additional thermal treatment.

Density Determinations

The densities of the partially and fully cured specimens at 24.95 ± 0.05°C (hereafter, 25°C) were measured using a density gradient column (ASTM D1505)[29] prepared using toluene and carbon tetrachloride.[1] The column was calibrated with density floats of 1.21053, 1.21477, 1.21953, and 1.22447 g/mL. Density measurements commenced approximately 10 min after the additional thermal treatment in the TBA oven, described above. Two to four disk specimens with the same cure history were placed individually into the column at approximately 5-min intervals. The position of each disk in the column was recorded vs. time. Each specimen, after an initial rapid descent in the column, equilibrated at a definite level in the column and maintained that level for at least 40 min. The position at 20 min was used to determine the reported density of each specimen. Reported densities for each value of conversion are the average of the two to four specimens.

DSC Experiments

Differential Scanning Calorimetric (DSC) experiments were used to determine T_g, the extent of physical aging, and Δc_p (the difference in heat capacities of the liquid or rubbery state and the glassy state) of the specimens. The glass transition appears as an endothermic shift over a temperature interval in the DSC heating scan. The value of T_g was taken as the midpoint of the step transition. The value of Δc_p was taken as the difference between the extrapolated liquid or rubbery state and glassy state heat capacity vs. temperature data at the defined T_g.

A physically aged specimen displays an endothermic peak, generally centered in a range from approximately T_g to $T_g + 10$°C. The area under this peak, with a baseline constructed from the extrapolated c_p vs. temperature data in the liquid or rubbery state, was used as an estimate of the extent of physical aging that had occurred within the specimen. No specimen used for measurements of density or thermal expansion coefficients displayed measurable aging peaks.

A differential scanning calorimeter capable of controlled cooling to −40°C was used for all DSC experiments (Perkin–Elmer DSC-4). The DSC oven was purged with dry nitrogen. The weighed specimens (mass approximately 10 mg) were contained in weighed and sealed aluminum DSC pans. DSC measurements were performed on specimens after curing in the large oven and after additional thermal treatment in the TBA oven (the temperature and atmosphere of which were closely controlled). Only the values of T_g of the specimens that had been cured in the larger oven and had experienced the additional thermal treatment in the TBA oven are reported here. A specimen was placed in the DSC unit at 25°C and cooled to −30°C at a programmed rate of 320°C/min. It was then subjected to a temperature scan from −30°C to $T_g + 40$°C, at a heating rate of 10°C/min.

Thermal Expansion Coefficient Determinations

Thermal expansion coefficients of specimens for each cure condition were determined using an automated dynamic mechanical analyzer of solid materials (Rheometrics Solid Analyzer RSAII). A rectangular specimen (dimensions 0.6 × 5.7 × 22.6 mm^3) was mounted at room temperature in the unit using the thin-film fixture. (No dynamic mechanical tests were performed using the unit.) The atmosphere was flowing dry nitrogen.

The specimen was then heated to approximately 20°C above T_g and then immediately cooled to 30°C at 5°C/min. This procedure was an attempt to relieve stresses that may have developed by curing in the aluminum mold. The specimen was then heated

at 5°C/min from 30°C to T_g + 20°C and then immediately cooled at 5°C/min to 30°C; data collected during this cooling ramp were used for the determination of the thermal expansion coefficients both above and below T_g. The value of T_g of each specimen was that taken using the corresponding DSC specimens.

The RSAII unit was programmed to keep the specimen under 10 g of tension (approximately 3 $\times 10^5$ dyne/cm^2) during the heating and cooling ramps by automatic continuous adjustment of the positions of the thin-film fixture clamps. The change in position of the clamps was recorded vs. temperature and the data obtained were used to determine the linear dimension (length) of the specimen vs. temperature.

RESULTS AND DISCUSSION

Principal Parameters of Epoxy–Amine Systems

The TBA technique was used to determine the principal transition temperatures from the maxima of aG'' vs. temperature at approximately 1 Hz for the systems under investigation; the transition temperatures are included in Table I. T_{g0} and $T_{\gamma 0}$ are the glass-transition temperature and secondary glassy-state transition temperature of the uncured material, respectively. The β-relaxation was not evident in the uncured material. $T_{g\infty}$ and $T_{\beta\infty}$ are the glass-transition temperature and secondary glassy-state transition temperature of the fully cured material, respectively. The γ-relaxation was evident only as a low-temperature shoulder on the β-relaxation damping peak in the fully cured material. It is noted that full cure in all of the systems involves complete reaction of all of the epoxy groups: for those systems with amine hydrogen/epoxy < 1/1 (i.e., r = 0.9 and 0.8) this involves reaction of excess epoxy with hydroxyl groups.[22]

Values for X_{gel}, the fractional conversion at molecular gelation as calculated using Flory's theory,[30,31] are included in Table I. ${}_{gel}T_g$ is defined as the value of T_g at a conversion corresponding to molecular gelation. The values of ${}_{gel}T_g$ in Table I were obtained from T_g vs. conversion data, obtained by DSC, previously reported from this laboratory.[20–22] ${}_eT_g$(min) is the minimum value of the glass-transition temperature (measured by TBA) at which the isothermal modulus of a material at any temperature passes through a maximum with increasing conversion (see later).

The principal parameters of T_{g0}, $T_{\gamma 0}$, $T_{g\infty}$, $T_{\beta\infty}$, X_{gel}, ${}_{gel}T_g$, and ${}_eT_g$(min) provide a framework for developing an understanding of the complex behavior of the properties of thermosetting systems after cure vs. chemical conversion.

In a previous report originating from this laboratory,[7,8] no distinction was made between the γ-relaxation and the β-relaxation; both relaxations were referred to as the β-relaxation. For completeness, in this report, the γ-relaxation and β-relaxation have been identified separately (see later).

In the following discussion, the T_g is used in two ways: as an actual value of temperature used to define the glass to rubber (or liquid) relaxation at approximately 1 Hz; and as a property of a specimen that measures the conversion of epoxide. T_g is used as a direct measure of conversion based on the one-to-one relationship between T_g and conversion.[20–23]

Data from TBA Experiment

Examples of the relative rigidity and relative out-of-phase shear modulus data for the stoichiometric system (r = 1.0) at three different conversions are shown in Figure 3. The vertical down arrow identifies the γ-relaxation and the vertical up arrow identifies the β-relaxation for the material with T_g = 64°C.

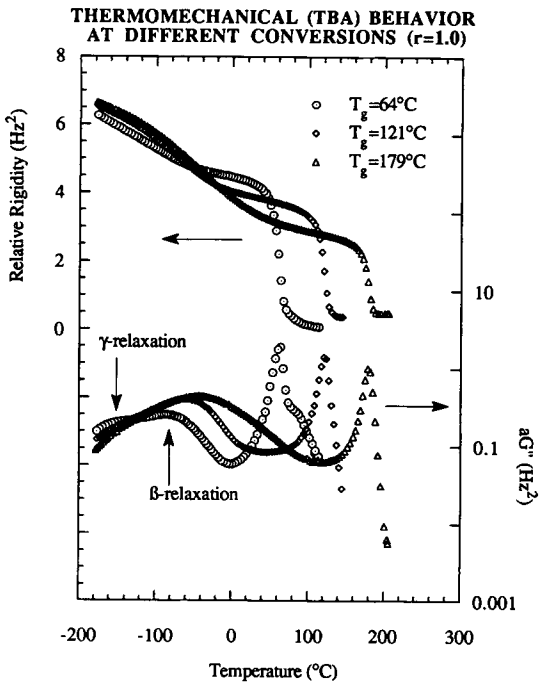

Figure 3 Thermomechanical (TBA) behavior of stoichiometric system (r = 1.0) at three different conversions. Data were collected on cooling (see text). Vertical arrows mark peaks in the aG'' data below T_g that correspond to the γ-relaxation and β-relaxation for the specimen with T_g = 64°C.

The intensity of the γ-relaxation weakens with increasing T_g; the γ-relaxation is scarcely apparent for $T_g = 179°C$.

The β-relaxation is apparent only at conversions higher than gelation, or equivalently at $T_g > {}_{gel}T_g$. All of the data shown in Figure 3 is of gelled material (${}_{gel}T_g$ for $r = 1.0$ system is 42°C, Table I). The temperature T_β increases with increasing T_g.

The isothermal modulus after cure may either increase, decrease, or experience a maximum with respect to conversion at a fixed temperature (e.g., $T = -140$, 20, 80°C, respectively, in Fig. 3). The isothermal modulus is also expected to increase in the rubbery state with increasing conversion. In the following analysis the relative rigidity data at different isothermal temperatures are plotted vs. conversion, as measured by T_g. Data at particular temperatures were obtained by interpolation of data obtained during cooling. (The corresponding mechanical loss data are not reported.)

All isothermal modulus data reported was obtained on cooling. It is noted that for the ungelled material, microcracking generally occurred at temperatures below −100°C. (Microcracking could be inferred from the hysteresis between cooling and heating data for a fixed conversion.) For this reason isothermal modulus vs. conversion data of ungelled material are shown only for $T > -100°C$. However, because microcracks did not appear to occur for gelled material, isothermal modulus data of gelled material are included for $T < -100°C$. A microcracked specimen could be "healed" (i.e., the microcracks removed) by heating to just below, as well as to above, T_g.

Secondary Relaxation Temperatures (T_γ and T_β) vs. T_g

In Figure 4, temperatures T_γ and T_β are plotted vs. T_g. At low conversions only the γ-relaxation peak is apparent. At high conversions the β-relaxation peak is pronounced whereas the γ-relaxation is only detected as a weak shoulder on the low-temperature side of the β-relaxation peak. As reported previously,[7,8] T_β is approximately linearly related to T_g at conversions above those corresponding to gelation.

The temperature values of $T_{\gamma 0}$ for the systems with $r = 1.2$, 1.0, 0.9, and 0.8 are −156, −155, −156, and −156°C, respectively. This suggests that the temperature location of the peak in the relative out-of-phase shear modulus of the γ-relaxation (which is related to its activation energy at constant frequency[32]) is independent of the initial ratio of amino hydrogens to epoxy groups in the systems. The decrease in intensity of the γ-relaxation peak with increasing conversion suggests that either the entities involved in the relaxation are becoming depleted with increasing conversion or that the developing network structure hinders the γ-motion.

Unlike the values of T_γ, the values of T_β show systematic variations with respect to the initial ratio

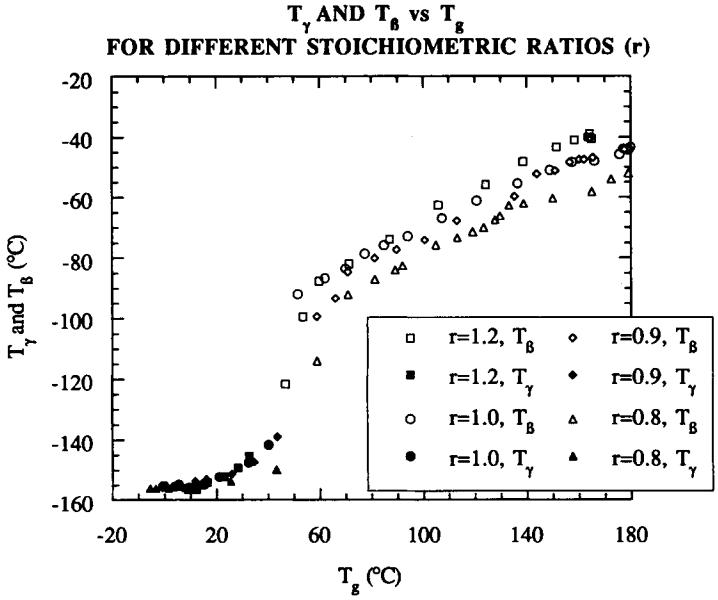

Figure 4 T_γ and T_β vs. T_g for different stoichiometric ratios. The filled and unfilled symbols correspond to T_γ and T_β, respectively (see text).

of amino hydrogen atoms to epoxy groups (Fig. 4). In general, the value of T_β at a given T_g (i.e., conversion) increases with an increasing ratio of amino hydrogen to epoxy groups (increasing r). This implies that the temperature location of the peak in the relative out-of-phase shear modulus of the β-relaxation (which is related to its activation energy at a constant frequency) is sensitive to the molecular structure or composition of the developing network.

For the epoxy-rich formulations, $r = 0.9$ and 0.8, T_β vs. T_g data show a relatively abrupt increase in the range $130 < T_g < 160$°C that is not observed for the other two systems (Fig. 4). This is a consequence of the epoxy reaction with hydroxyl that occurs in epoxy-rich systems to produce an ether linkage with additional crosslinks.[22] It has been shown that in the DGEBA/TMAB system with $r = 0.8$, the epoxy-hydroxyl reaction occurs after the depletion of amino hydrogens at a conversion value corresponding to a T_g value equal to 120°C.[22] This implies that the epoxy–hydroxyl reaction has a different affect on the β-relaxation than the epoxy–amine reactions as a consequence of the different structures in the developing network.

Modulus vs. T_g($T < -80$°C)

The relative modulus, defined as the relative rigidity of the material at any state of cure divided by the relative rigidity of the uncured material, is plotted in Figure 5 vs. T_g at $T = -90$°C for the systems with different stoichiometries. The data in Figure 5 have been shifted vertically by multiple intervals of 0.05 for clarity (data for $r = 1.2$ have not been shifted).

The isothermal modulus at −90°C vs. T_g sets of data appear to be linear in two conversion regions separated by the value of ${}_{gel}T_g$, the pre-gel data having a higher slope than the post-gel data. This behavior has been reported to occur at temperatures from −180 to −80°C for the DGEBA/TMAB $r = 1.0$ system.[7,8] (No physical significance was attributed to the temperatures of −80 and −180°C.)

The increase in isothermal modulus below T_g may arise for the following reasons: as the sub-T_g relaxation transitions rise to above T the relaxations of the transitions freeze out; the increasing concentration of hydroxyl groups in the system with increasing conversion increases the attractive forces (i.e., hydrogen bonding) between submolecular groups; and microcracking, on cooling to T from above T_g, could be more severe the lower the T_g (i.e., the lower the conversion).

Modulus vs. T_g(-80°C $< T < T_{g0}$)

The behavior of the isothermal modulus after cure vs. T_g in the temperature region, -80°C $< T < T_{g0}$, is more complicated than below approximately −80°C (e.g., $T = -90$°C, as above). An example is displayed in Figure 6 for the system with $r = 1.0$ for several temperatures (−80, −60, −40, and −20°C). The other formulations ($r = 0.8$, 0.9, and 1.2) followed the same pattern in this temperature range. The modulus passes through a maximum and then a minimum with increasing T_g for some temperatures (−60, −40, and −20°C). The maximum is independent of the temperature and occurs near ${}_{gel}T_g$. The maximum in isothermal modulus below T_{g0} vs. conversion may be due to the competition of factors, which increase the modulus (as above), with relaxational or structural factors that reduce the modulus with increasing conversion (see later).

It has been implied in previous work[7,8] that the minimum is due to T_β passing through the isothermal temperature with increasing conversion. The value of $T_\beta = T$ is marked by the filled down arrows in Figure 6. Note that the conversion at which $T_\beta = T$ does not correspond directly to the minimum in modulus for the data shown in Figure 6. The increase in the concentration of hydroxyl groups, and thus hydrogen bonding, may contribute to the increase in isothermal modulus vs. conversion before $T_\beta = T$. More generally, there are likely to be offsets between assignments of minimum and maximum values of isothermal properties and transitional assignments with increasing conversion since whereas the maxima and minima may correspond to a relaxation having completely passed through the measurement temperature with increasing conversion, the assignment of the relaxation (e.g., of T_g, T_β . . .) is not usually made at the end of a relaxation but, for example, from maxima in G' or tan δ.

Modulus vs. T_g($T_{g0} < T < T_{g\infty}$)

At isothermal temperatures for which $T_{g0} < T < T_{g\infty}$ the material experiences the effects of the transformation from liquid to glass (i.e., vitrification) with increasing conversion (T_g). The modulus of the material with $r = 1.0$ at 25°C vs. T_g is shown in Figure 7. The other formulations ($r = 0.8$, 0.9, and 1.2) followed the same pattern at this temperature. As T_g of the cured material passes through the isothermal temperature the modulus rapidly rises. As the glass transition rises above a given isothermal temperature above T_{g0}, the relaxations of the transition

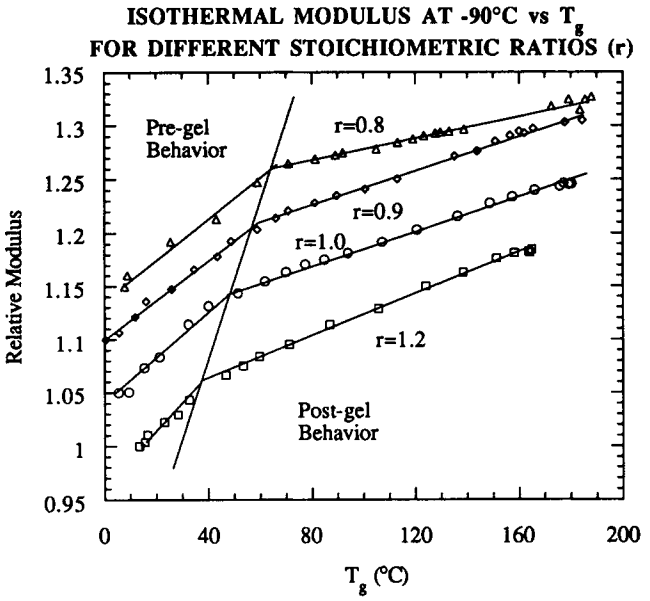

Figure 5 Isothermal modulus vs. T_g at $T = -90°C$. The lines are visual aids only.

freeze out causing the isothermal modulus to increase. As T_g further increases above 25°C the modulus reaches a maximum value and then decreases with increasing T_g. The decreasing modulus is attributed to the increased hindrance of the more extensively crosslinked and higher molecular weight system to densify and pack tightly.

This decrease in isothermal modulus in the glassy state, after cure and cooling through T_g, with increasing conversion may be due to structural effects, i.e., that increasing crosslinks and increasing molecular weight prevent efficient structural packing even in the equilibrium state (which would be realized after infinite time), or due to relaxational (kinetic) effects, i.e., that increasing crosslinks and increasing molecular weight decrease the rate at which the glass densifies in an attempt to achieve its equilibrium configuration on cooling through the glass

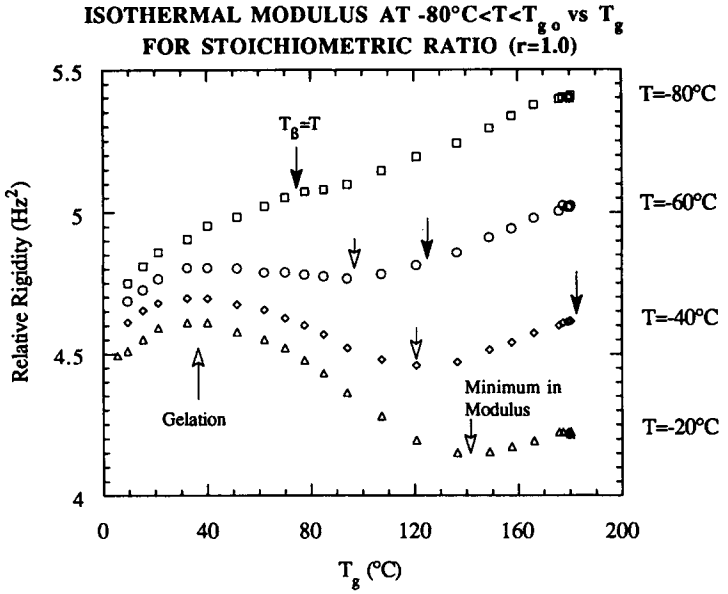

Figure 6 Isothermal modulus vs. T_g for stoichiometric system ($r = 1.0$) for values of $T = -80, -60, -40$, and $-20°C$. The downward pointing filled arrows mark T_g. The downward pointing unfilled arrows mark minimum in modulus vs. conversion. The upward pointing unfilled arrow marks molecular gelation.

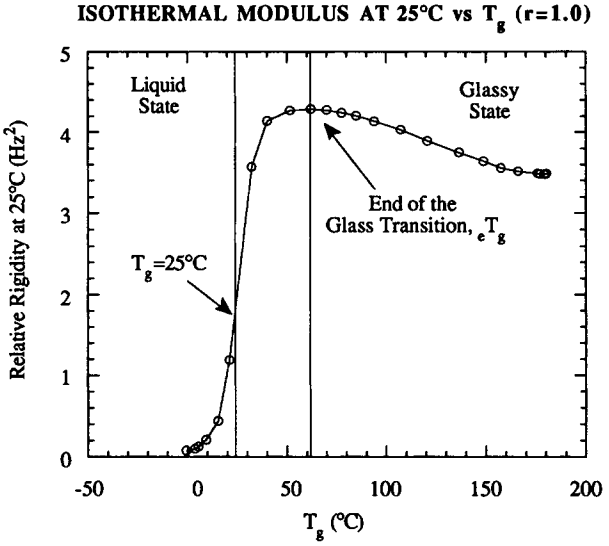

Figure 7 Modulus vs. T_g at 25°C for stoichiometric (r = 1.0) system.

transition to the isothermal temperature of measurement. The relative contributions of structural and relaxational factors is not presently well understood, but is a key issue in the understanding of the glassy state properties of thermosetting systems. The structural argument would lead to the isothermal modulus at a cure temperature in the equilibrium rubbery state (e.g., for cure temperature greater than $T_{g\infty}$) eventually decreasing with increased conversion. If this is found not to be true, the decrease in the isothermal glassy state modulus after cure with increasing conversion would then presumably be the consequence of relaxational (kinetic) effects on cooling through T_g to the temperature of measurement.

The value of T_g at which the isothermal modulus is at a maximum value is denoted as $_eT_g$. $_eT_g$ is considered to be related to the value of conversion at which the entire glass relaxation peak has passed above the measurement temperature. At the conversion at which the entire glass relaxation has risen above the temperature, no further increases in modulus are realized by the vitrification process. Further increased crosslinks and increased average molecular weight with increased conversion are considered to decrease the packing ability of the glass and decrease the modulus. The isothermal modulus is displayed for several values of $T > T_{g0}$ for the r = 1.0 material in Figure 8. The other formulations (r = 0.8, 0.9, and 1.2) followed the same pattern in this temperature range. It is anticipated and it is observed that $_eT_g$ increases with increasing T for $T > T_{g0}$.

On the basis of the explanation for the maximum in the isothermal modulus vs. conversion for $T > T_{g0}$ being from competition between the effect of vitrification on cooling from above T_g to T (which increases the modulus) and the decreasing packing ability (which decreases the modulus), it follows that vitrification would play no role for isothermal temperatures sufficiently below the T_{g0} (e.g., at T = −60°C). On this basis, the maximum in isothermal modulus that is observed at −60°C in the vicinity of gelation (Fig. 6) is the consequence of factors other than vitrification.

The values of $_eT_g$ for the systems with different values of r are plotted on the plane formed using T_g and T as coordinates in Figure 9. Data of $_eT_g$ vs. T_g for the different stoichiometric systems overlap at high conversion; the values of $_eT_g$ for the different systems depart from the apparent single locus at low conversions. The lowest value of $_eT_g$ for each value of r is denoted as $_eT_g$(min) and appears to occur in the vicinity of $_{gel}T_g$ (see Table I). This suggests that gelation plays a role in the maximum in modulus with increasing conversion and that the anomaly (as observed in the isothermal modulus decreasing with increasing conversion) only occurs in the gelled material for the present system.

A question arises to whether the variations in $_eT_g$(min) for the systems with different values of r are caused by the different values of T_{g0} in the systems or whether they are caused by the phenomenon of gelation as measured by $_{gel}T_g$. It might be argued that if the value of T_{g0} determined the value of $_eT_g$(min) for each system, assuming that $_eT_g$(min)

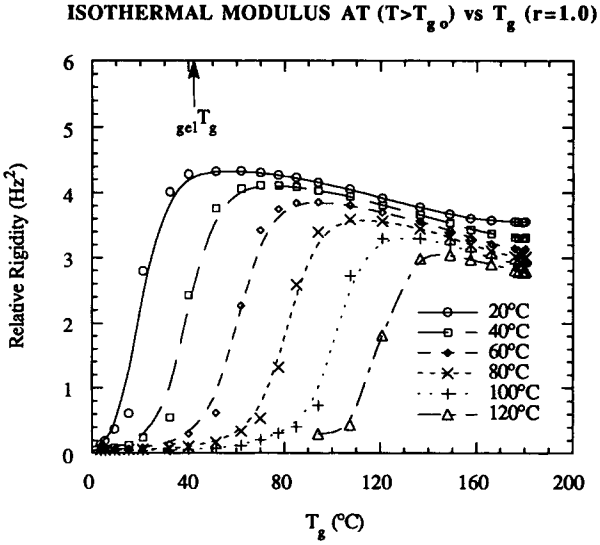

Figure 8 Isothermal modulus vs. T_g for values of $T > T_{g0}$ for stoichiometric system (r = 1.0).

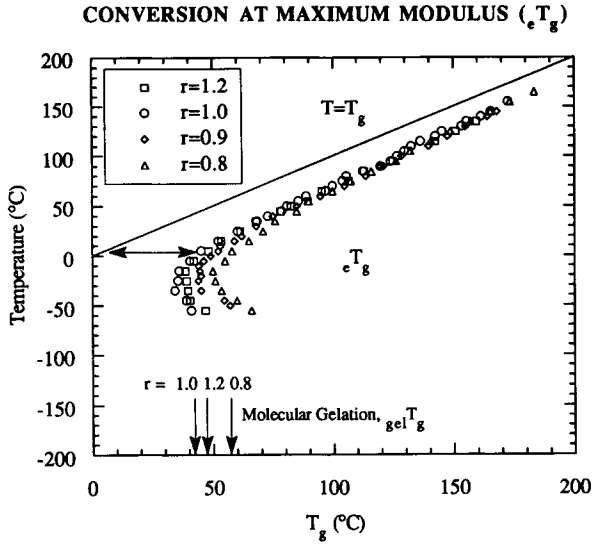

Figure 9 Maximum of isothermal modulus, $_eT_g$, vs. conversion (T_g) plotted on T_g and T coordinates. Molecular gelation conversions, as marked by $_{gel}T_g$, were obtained using DSC.[20-22] The horizontal double-headed arrow indicates the value in (°C) of $_eT_g - T_g$ at $T = 4$°C for $r = 1.0$.

was a constant amount higher than T_{g0} for all the systems with different values of r, an increase in T_{g0} would dictate an increase in $_eT_g$(min).

Note that the value of $_eT_g$(min) increases in the following order: $r = 1.0$, $r = 1.2$, $r = 0.9$, and $r = 0.8$ (Table I). For the values of $_{gel}T_g$ that have been obtained, $_{gel}T_g$ increases in the following order: $r = 1.0$, $r = 1.2$, and $r = 0.8$ (Table I). The value of T_{g0} increases in the following order: $r = 0.8$, $r = 0.9$, $r = 1.0$, and $r = 1.2$ (Table I). It is observed that $_eT_g$(min) is not a constant amount higher than T_{g0} for the systems studied here. There is, however, a positive correlation between the values of $_{gel}T_g$ and $_eT_g$(min). Thus, these data imply that the value of $_eT_g$(min) is related to the conversion corresponding to gelation (i.e., $_{gel}T_g$) rather than to the value of T_{g0} of a system.

The values of $_{gel}T_g$ are approximately 7°C greater than the corresponding values of $_eT_g$(min). This mismatch might partially arise because the values of $_{gel}T_g$ were obtained from DSC data using Flory's theory for molecular gelation[20-22]; the values of $_eT_g$(min) were obtained from torsion pendulum data that correspond to macroscopic measurements.[27,33]

It has been stated in a previous report[7,8] that the conversion interval, $_eT_g - T_g$ (where $T_g = T$) is a constant with respect to conversion and equal to approximately 35°C for the DGEBA/TMAB system with $r = 1.0$. [To determine the value of $_eT_g - T_g$ in Fig. 9, choose a value of $_eT_g$ (read off the x-axis) and the corresponding value of $T_g = T$ horizontally to the left of $_eT_g$.] However, this report, using more measurements and different stoichiometric ratios shows that $_eT_g - T_g$ decreases with increasing T_g at high T_g.

For $T > T_{g0}$, as stated above, $_eT_g$ is related to the conversion at which the entire glass relaxation region rises above the measurement temperature. The magnitude of $_eT_g - T_g$ can then be related to the breadth of the glass relaxation vs. temperature. This is in accordance with data collected (e.g., see Fig. 3). For high T_g material the glass relaxation peak in terms of relative loss modulus is relatively narrow and $_eT_g - T_g$ is observed to be small. For material with an intermediate T_g, the glass relaxation peak is broad and $_eT_g - T_g$ is observed to be larger. For the DGEBA/TMAB system, the glass relaxation peak is relatively narrow also for very low T_g ($T_g < {}_{gel}T_g$) material (data not shown); however, an assignable value for $_eT_g$ was absent because no maximum in modulus vs. conversion is observed at any temperature for conversions less than the conversion corresponding approximately to gelation. The breadth of the T_g region for different conversions reflects the dispersity of molecular structure. The dispersity of molecular structure of a DGEBA/TMAB system is less for unreacted ($T_g = T_{g0}$) and for fully reacted ($T_g = T_{g\infty}$) material than for material at intermediate conversions.

T_gTP Diagram

A T_gTP diagram has the T_g as the x-axis, T as the y-axis, and a property, P, as the projection from the implied third orthogonal axis onto the plane formed by T_g and T.[7,8,12,13] The diagram can include transition temperatures such as T_g, T_β, and T_γ vs. conversion (T_g) to relate properties to the transitions. Maximum, minimum, and iso-value contours of the property also can be projected onto the plane formed by T_g and T. The diagram can explicitly show the effect of increasing conversion (T_g) on the isothermal properties of a thermoset, the effect of temperature at a fixed conversion, as well as the influence of transitions as they pass through the isothermal temperature of measurement in terms of different regions of behavior.

Isothermal modulus vs. T_g data for the four stoichiometric systems were used to construct a T_gTP diagram with modulus as the property (P) in Figure 10. The vitrification line is defined as $T = T_g$. Above $T = T_g$ the material is a liquid before gelation and a rubber after gelation. Below $T = T_g$ the material

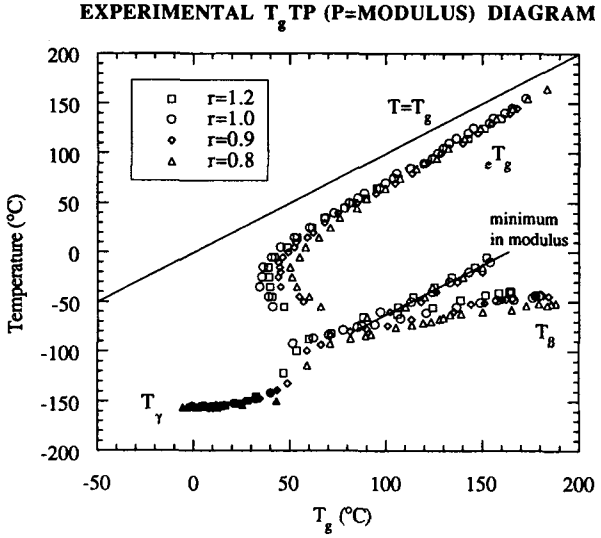

Figure 10 Experimental data (maxima and minima in isothermal modulus, and T_γ and T_β) for the four systems (r = 1.2, 1.0, 0.9, and 0.8) plotted on a T_gTP (P = modulus) diagram.

is a glass. Prior to gelation the glass is brittle, after gelation the glass becomes tougher with increasing conversion.

Values of ${}_eT_g$ are included in Figure 10. The values of ${}_eT_g$ for the different stoichiometries overlap at conversions $T_g \gg {}_{gel}T_g$. In this range ${}_eT_g$ depends mainly on the value of T_g. At lower values of T_g, the maxima depart from the single contour. As stated above, the minimum values of ${}_eT_g$ at which the maxima in isothermal modulus are observed, ${}_eT_g$(min), correspond approximately to molecular gelation, ${}_{gel}T_g$.

Also displayed in the T_gTP diagram of Figure 10 are the values of $T = T_\gamma$ and $T = T_\beta$ vs. T_g. At temperatures lower than the sub-T_g relaxations, i.e., T_γ and T_β, the material is relatively more brittle than at temperatures above the sub-T_g relaxations. The material is also significantly more brittle in the glassy state at conversions less than the conversion at gelation. This brittleness may be observed in the TBA experiment via the phenomenon of microcracking (as discussed earlier).

Also plotted on the T_gTP diagram of Figure 10 are the values of the minimum in isothermal modulus for the temperature range $-80°C < T < T_{g0}$ for the stoichiometries investigated; the data fall on one line within the scatter of the data. The line drawn in Figure 10 represents the locus of these minimum values. This line is approximately parallel to $T = T_g$, suggesting a dependency on T_g rather than T_β (as previously reported[7,8]).

Not shown on the T_gTP diagram of Figure 10 are the conversions at which the isothermal modulus vs. T_g data change slope (as for $T = -90°C$ in Fig. 5). These conversions correspond approximately to gelation for the stoichiometries and measurement temperatures investigated (see Fig. 5).

From the above results it follows that the conversion corresponding to gelation affects the location (or existence) of ${}_eT_g$ at values of conversion near gelation (near ${}_{gel}T_g$); at higher conversions the position of ${}_eT_g$ is related only to the vitrification process. An empirical shift factor based on the value of ${}_eT_g$(min), which has been correlated with ${}_{gel}T_g$, is utilized to collapse the data onto a single locus in the normalized T_gTP diagram (Fig. 11). The shift factor is:

$$a_{eT_g} = [{}_eT_g(\text{min}, ref) - {}_eT_g(\text{min})] \times \exp\left[\frac{({}_eT_g(\text{min}) - T_g)°C}{({}_eT_g(\text{min}, ref))°C}\right] \quad (4)$$

where ${}_eT_g$(min, ref) is taken as that of the r = 0.9 system. The first factor on the right hand side of eq. (4) is the full shift with respect to the differences in ${}_eT_g$(min) between the reference material and a material with a different value of r; the exponential factor is a non-optimized weighting factor that reflects the larger influence of gelation on the values of ${}_eT_g$ at lower conversions. The weighting factor approaches 1 when T_g approaches ${}_eT_g$(min) and approaches 0 as T_g becomes much greater than ${}_eT_g$(min). The same shift factor is utilized and is

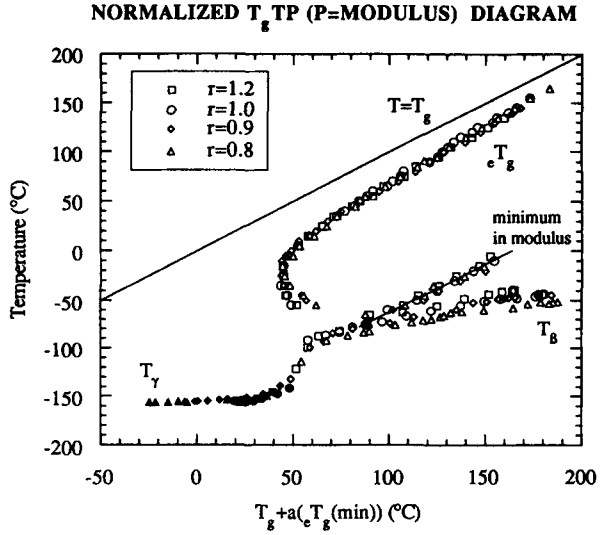

Figure 11 Shifted data of Figure 10 plotted on a normalized T_gTP (P = modulus) diagram (see text).

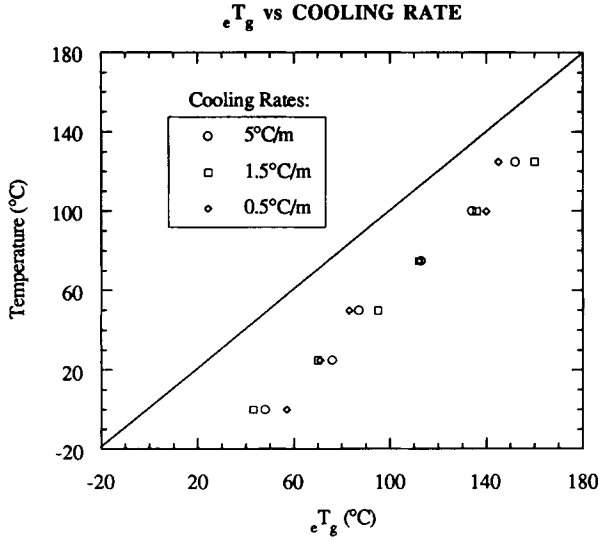

Figure 12 $_eT_g$ values for different cooling rates (r = 1.0).

adequate for the values of $_eT_g$, T_γ, and the minimum in modulus. The shifted values of T_β, however, show differences at high conversions before and after shifting.

Figure 12 shows values of $_eT_g$ for data collected on the DGEBA/TMAB system with r = 1.0 taken at different cooling rates. The scatter in the data prohibits any conclusion being made on the effect that the cooling rate has on the location of $_eT_g$ in the temperature-conversion plane.

T_gTP Diagrams for Other Thermosetting Systems

Similar T_gTP (P = modulus) diagrams, as for those for the DGEBA/TMAB systems, have been constructed for a dicyanate ester to polycyanurate system (crosslinked network)[12] and a polyamic acid ester to polyimide system (linear semiladder polymer).[13] Despite significant differences in chemical structure, the glassy state material properties display similar general phenomena with respect to increased conversion. One similarity is a locus of values of $_eT_g$ that is linear with increased conversion at high conversions and has values of $_eT_g - T_g$ in the order of 20–60°C. Also similar for the DGEBA/TMAB and dicyanate ester to polycyanurate crosslinking systems is the abrupt change in behavior of the glassy-state relaxations at conversions near gelation.

There are, however, some interesting differences. For example, with the dicyanate ester to polycyanurate system at measurement temperatures below T_{g0}, the isothermal modulus decreases with respect to increasing conversion throughout the entire conversion range. The decrease in the isothermal modulus with increasing conversion in the dicyanate ester system at low temperatures has been attributed to a decreased ability of the material to pack in the glassy state.[12] (This is suggested by the concept that monodispersed monomers can pack more effectively than a distribution of higher molecular weight material.) In contrast, for epoxies, an increase in isothermal modulus with increasing conversion is observed at temperatures less than T_{g0}.

The polyamic acid ester/polyimide T_gTP diagram also shows the anomalous behavior of the isothermal modulus decreasing with conversion at $T > T_{g0}$.[13] However, the isothermal modulus vs. conversion at low temperatures for the polyimide system is more complicated. The behavior below T_{g0} for the polyimide system analyzed may be a consequence of the existence of three sub-T_g relaxations; the three relaxations experience changes in both intensity and in value of the relaxation temperature vs. conversion. Experimental complications arise in the polyimide system due to a loss of mass during cure that changes the dimensions of the specimen and negates the proportionality between the relative rigidity and modulus. The mass loss also changes the relative concentrations of atoms such as carbon, oxygen, nitrogen, and hydrogen of the system.

Dilatometric Findings

The density at 24.95 ± 0.05°C for the stoichiometric DGEBA/TMAB system (r = 1.0) versus conversion, T_g, is displayed in Figure 13. The values of T_g for the specimens were determined by DSC as outlined in Experimental (also see next section). As for the

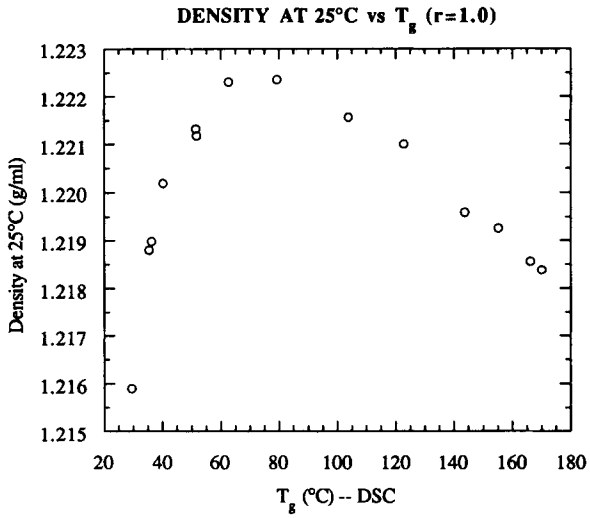

Figure 13 Density of stoichiometric system (r = 1.0) at 24.95 ± 0.05°C vs. T_g.

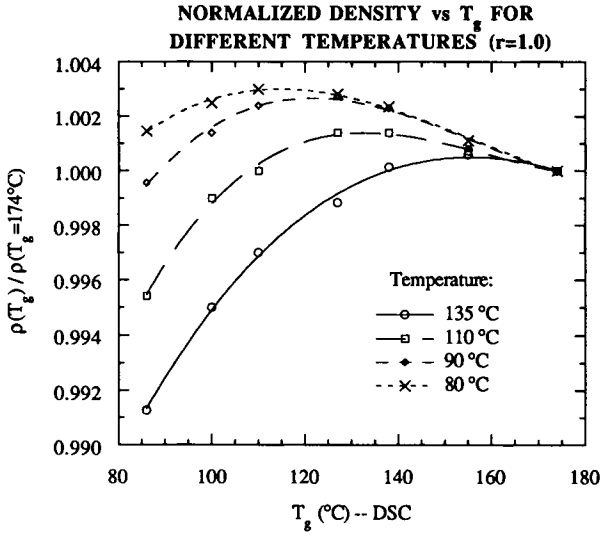

Figure 14 Normalized density of stoichiometric system (r = 1.0) vs. T_g for $T > T_{g0}$.

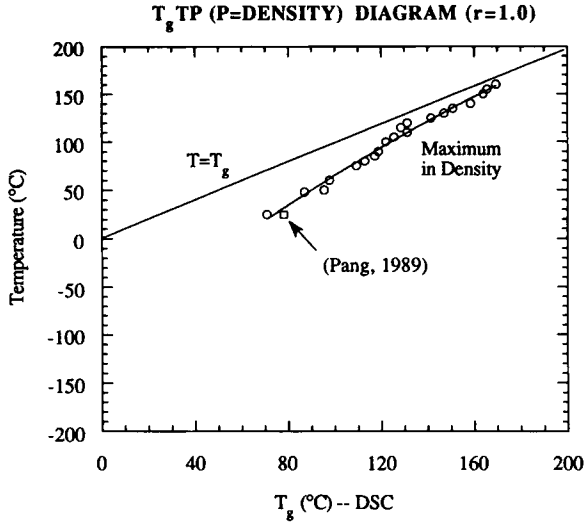

Figure 15 T_gTP diagram with density as the property (r = 1.0).

modulus data, the density increases as T_g passes through T, reaches a maximum at $T_g > T$, and then decreases as T_g increases further.

The density of the specimens at isothermal temperatures other than 25°C was determined by using the density at 25°C and the thermal expansion coefficients of the rubbery and glassy states for a given conversion. Figure 14 displays normalized density (i.e., density at a given T_g divided by the density of the material at a conversion corresponding arbitrarily to T_g = 174°C) vs. T_g data for different values of T. It is observed that the maximum in density vs. conversion (i.e., ${}_eT_g$ via density data) increases with increases in T. In analogy with Figure 9, a limited T_gTP diagram with P = density is plotted in Figure 15. Note that like the modulus data at conversions above gelation and $T > T_{g0}$, the locus of ${}_eT_g$ data points via density falls approximately on a straight line and that the value of ${}_eT_g - T_g$ measured via density decreases with increasing conversion (T_g).

The modulus and the density at 25°C are plotted for comparison in reduced forms vs. T_g in Figure 16 (reduced form is defined as the difference between the value of the property at a conversion of T_g and the maximum value of the property divided by the maximum value of the property). The values of T_g for the modulus data were acquired using TBA and the values of T_g for the density data were acquired using DSC; use of different techniques to determine T_g will tend to weaken the correlation. The modulus and density sets of data show similar behavior. Note that the multiplicative factor of 60 (a non-optimized factor) is used to magnify the changes in reduced density and results in superposition of the density data with the modulus data.

The data in Figure 16 suggest that the value of the modulus at 25°C is dominated by the density (i.e., packing) at 25°C and that small changes in density correlate with relatively large changes in modulus. Data at other temperatures above T_{g0} (e.g., density data in Fig. 14) show agreement (not shown explicitly) between the density and modulus. Therefore, for these results, the modulus is demonstrated to be a convenient and sensitive property that reflects the behavior observed in the isothermal density with increasing conversion for conversions

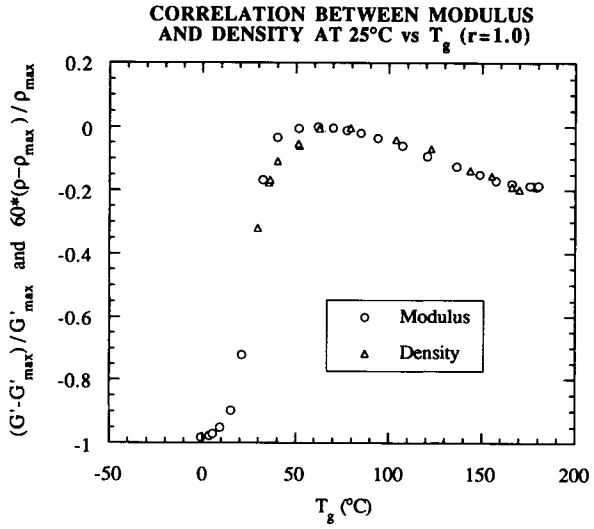

Figure 16 Reduced modulus and reduced density at 25°C vs. T_g for r = 1.0.

greater than gelation and temperatures greater than T_{g0}.

It has been suggested that the isothermal free volume after cure vs. T_g passes through a minimum value with increasing conversion.[1] Such changes in free volume with conversion above T_{g0} would account for the maximum in density and in modulus with conversion. Positron annihilation spectroscopy[34] experiments on the DGEBA/TMAB system with r = 1.0 have provided information on the free volume concentration and average radius size of free volume holes vs. conversion in the DGEBA/TMAB system with r = 1.0.[26,35] Results show that the fractional free volume of specimens at 25°C passes through a minimum value vs. conversion. The conversion corresponding to the minimum in fractional free volume at 25°C is the same as for the maximum in density and modulus at 25°C.

T_g vs. Conversion Relationship

The preceding work relies on the T_g vs. conversion relationship being a one-to-one relationship; this allowed T_g to be used as a direct measure of conversion. Evidence for this appears in previous work on the DGEBA/TMAB system[20–24] as well as in work performed on other thermosetting systems.[36,37]

The T_g vs. conversion data for the DGEBA/TMAB stoichiometric system (r = 1) included in Figure 17 are for different time–temperature cure conditions.[20,21] The values of conversion and T_g were determined from a DSC heating scan at 10°C/min on unaged specimens cured to different extents. It is realized that the system may not truly achieve full cure (i.e., 100% of the epoxide groups reacted) for the cure schedule used in this study[38]; however, the maximum conversion observed and its corresponding T_g are denoted as x = 1 and $T_g = T_{g\infty}$, respectively.

Note that the data at different cure temperatures overlap, suggesting a unique relationship between conversion as measured by the residual heat in the DSC scan and T_g. Also note that the data are highly nonlinear and that the value of the slope is largest at the highest conversion. Thus, by plotting the material properties vs. T_g, as in the T_gTP diagram, the conversion axis at high conversions is expanded relative to those at low conversions.

Recent work has argued that the value of T_g is insensitive to the ratio of the extents of reaction of the different competing crosslinking reactions in a single aromatic amine/epoxy system.[24] According to this argument the value of T_g is related to the overall sum of the extents of the competing reactions in a

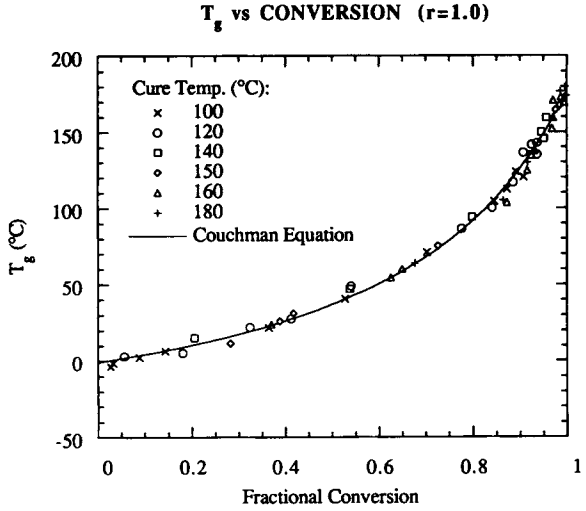

Figure 17 T_g vs. conversion data for the stoichiometric system (r = 1.0) of DGEBA/TMAB for different time–temperature cures.[20,21] The full line was constructed using eq. (6) with T_{g0} = 5°C, $T_{g\infty}$ = 178°C, and yields a best-fit value of $\Delta c_{p\infty}/\Delta c_{p0}$ = 0.37 (cf., direct experimental value of 0.35).

thermosetting system, assuming that each type of reaction increases T_g an equal amount. With this in mind, the value of T_g in this study is used here as an overall sum of all the reactions that have occurred. In this report, no attempt was made to distinguish the extents of different reactions in the systems.

Reports have been published on the DGEBA/TMAB reaction kinetics.[20–22,24] In the DGEBA/TMAB system with r = 1.0, epoxy groups react with primary and secondary amines. However, for the epoxy-rich DGEBA/TMAB system, etherification (i.e., the reaction between epoxide and hydroxyl groups) can occur.[22] As the data of Figure 11 demonstrate, the details of the extents of the different reactions do not seem to affect the loci of the values of ${}_eT_g$ beyond the manner that those reactions are reflected in the values of ${}_{gel}T_g$ and T_g of the systems.

The concept that T_g vs. conversion data are independent of the relative extents of different reactions in a system can be further demonstrated by fitting the data to an equation originally proposed by Couchman and Karasz[39,40] to predict the value of T_g for a polymer system vs. compositional variation:

$$\ln(T_g) = \frac{W_1 \ln(T_{g1}) + \dfrac{\Delta c_{p2}}{\Delta c_{p1}} W_2 \ln(T_{g2})}{W_1 + \dfrac{\Delta c_{p2}}{\Delta c_{p1}} W_2} \quad (5)$$

where W_1 and W_2 are the weight fractions of materials 1 and 2, T_{g1} and T_{g2} are the values of T_g of the homopolymers of material 1 and 2 in Kelvin, and Δc_p is the heat capacity of the liquid or rubber minus that of the glass of the homopolymers. The values of T_g and Δc_p can often be conveniently measured by DSC, leaving no adjustable parameters.

The Couchman equation has been modified for utilization in a crosslinking system to give[26,41]:

$$\ln(T_g) = \frac{(1 - x)\ln(T_{g0}) + \frac{\Delta c_{p\infty}}{\Delta c_{p0}} x \ln(T_{g\infty})}{(1 - x) + \frac{\Delta c_{p\infty}}{\Delta c_{p0}} x} \quad (6)$$

where x is the fractional conversion, and 0 and ∞ denote uncured and fully cured material. In the derivation of eq. (6) it was assumed that the system behaves as a random mixture of reacted and unreacted ends.

To test the applicability of this equation, the T_g vs. conversion set of data for the DGEBA/TMAB system with $r = 1.0$ (Fig. 17) was fit using T_{g0} and $T_{g\infty}$ values of -5 and 178°C measured independently by DSC and the value of $\Delta c_{p\infty}/\Delta c_{p0}$ was left as a fitting parameter to compare with the independently measured DSC value. It is shown in Figure 17 that the equation displays the nonlinear behavior effectively. Further, the best-fit value of $\Delta c_{p\infty}/\Delta c_{p0}$ was determined to be 0.37 which is equal (within the uncertainty of the data) to the independently DSC measured value of 0.35.[26,41] The quantitative agreement between the data and eq. (6) demonstrates the insensitivity of the T_g vs. conversion relationship to the various competitive reactions that take place in the DGEBA/TMAB system (for $r = 1.0$) and also provides support for the basis of the derivation of eq. (6).

In comparison with other equations that predict T_g vs. conversion data in thermosetting systems,[20-23,36,37,42] this equation has the advantages that: there are no adjustable parameters; for many thermosetting systems, verification can be conveniently performed by independently measuring the constants in the equation with only two DSC runs; the equation is relatively simple; and the single assumption that the system behaves as a random mixture of reacted and unreacted ends is reasonable and not restrictive.

CONCLUSIONS

1. Four diepoxy-tetrafunctional diamine formulations with different ratios of amino hydrogen atoms to epoxide groups exhibit maxima and minima in isothermal modulus vs. conversion (T_g) data. The maxima, which occur at a value of T_g denoted as ${}_eT_g$, can be correlated to the effects of gelation and vitrification.
2. A normalized conversion–isothermal temperature–property (T_gTP) diagram with modulus as the property was constructed for the four stoichiometric ratios. Normalization of the different systems was performed by shifting the data with respect to the conversion corresponding to the minimum value of ${}_eT_g$, denoted as ${}_eT_g$(min), for each system on the conversion axis and by using T_g as the conversion axis.
3. The density at 24.95 ± 0.05°C after cure passes through a maximum in the glassy state with increasing conversion (T_g). The density at higher isothermal temperatures after cure also passes through a maximum with increasing conversion.
4. The modulus after cure vs. conversion data for conversions greater than gelation and temperatures greater than T_{g0} reflect the density after cure vs. conversion behavior. The density vs. conversion behavior is presented in a T_gTP diagram (P = density). The measured percent changes in modulus vs. conversion are approximately 60 times greater than those in density.
5. The T_g vs. conversion relationship for the diepoxy-tetrafunctional diamine formulation with a stoichiometric ratio of amino hydrogens to epoxide groups is quantitatively predicted by an adaptation of the Couchman equation.

REFERENCES

1. K. P. Pang and J. K. Gillham, *J. Appl. Polym. Sci.*, **37,** 1969 (1989).
2. V. B. Gupta, L. T. Drzal, and M. J. Rich, *J. Appl. Polym. Sci.*, **30,** 4467 (1985).
3. D. A. Shimp and S. J. Ising, *35th Int. SAMPE Symp. and Exhib.*, **35,** Covina CA, April 1990, pp. 1045–1046.
4. A. Shimazaki, *J. Polym. Sci.*, **C23,** 555 (1968).
5. W. Fisch, W. Hofmann, and R. Schmid, *J. Appl. Polym. Sci.*, **13,** 295 (1969).
6. Y. G. Won, J. Galy, J. P. Pascault, and J. Verdu, *Polymer,* **32,** 79 (1991).

7. X. Wang and J. K. Gillham, *J. Coatings Technol.*, **64**(807), 37 (1992).
8. X. Wang and J. K. Gillham, *J. Appl. Polymer Sci.*, **47,** 425 (1993).
9. M. T. Aronhime, X. Peng, and J. K. Gillham, *J. Appl. Polym. Sci.*, **32,** 3589 (1986).
10. O. Y. Ol'khovik, *Vysokomol. Soyed.*, **A18**(5), 1012 (1976).
11. J. M. Charlesworth, *Polym. Eng. Sci.*, **28**(4), 230 (1988).
12. S. L. Simon and J. K. Gillham, *J. Appl. Polymer Sci.*, **51,** 1741 (1994).
13. R. A. Venditti, J. K. Gillham, E. Chin, and F. M. Houlihan, in *Advances in Polyimide Science and Technology,* C. Feger, Ed., Technomic Publishing, Lancaster, PA, 1992, pp. 336–350.
14. L. C. E. Struik, *Physical Aging in Amorphous Polymers and Other Materials,* Elsevier Sci. Publ., Amsterdam, 1978.
15. R. A. Venditti and J. K. Gillham, *J. Appl. Polymer Sci.*, **45,** 1501 (1992).
16. R. A. Venditti and J. K. Gillham, *J. Appl. Polymer Sci.*, **45,** 501 (1992).
17. G. Wisanrakkit and J. K. Gillham, *J. Appl. Polymer Sci.*, **42,** 2465 (1991).
18. S. L. Simon and J. K. Gillham, in *Chemistry and Technology of Cyanate Ester Resins,* I. Hamilton, Ed., Chapman and Hall, London, 1994, Ch. 4, pp. 87–111.
19. X. Wang and J. K. Gillham, *J. Appl. Polymer Sci.*, **47,** 447 (1993).
20. G. Wisanrakkit and J. K. Gillham, *J. Appl. Polymer Sci.*, **41,** 2885 (1990).
21. G. Wisanrakkit and J. K. Gillham, *J. Appl. Polymer Sci.*, **42,** 2453 (1991).
22. S. L. Simon and J. K. Gillham, *J. Appl. Polymer Sci.*, **46,** 1245 (1992).
23. X. Wang and J. K. Gillham, *J. Appl. Polymer Sci.*, **45,** 2127 (1992).
24. X. Wang and J. K. Gillham, *J. Appl. Polymer Sci.*, **43,** 2267 (1991).
25. J. K. Gillham and J. B. Enns, *Trends Polym. Sci.*, **2,** 406 (1994).
26. R. A. Venditti, Ph.D. Thesis, Department of Chemical Engineering, Princeton University, June 1994.
27. J. K. Gillham in *Developments in Polymer Characterisation,* J. V. Dawkins, Ed., Applied Science Pub. Ltd., London, 1982, pp. 157–227.
28. J. B. Enns and J. K. Gillham, *ACS Symp. Ser.*, **197,** 329–352 (1982).
29. ASTM Standards, Part 27, ASTM, Philadelphia, 1965, p. 500.
30. P. J. Flory, *Principles of Polymer Chemistry,* Cornell Univ. Press, Ithaca, NY, 1953.
31. D. R. Miller and C. W. Macosko, *Macromolecules,* **9**(2), 206 (1976).
32. J. Heijboer, *Intern. J. Polym. Mater.*, **6,** 11 (1977).
33. J. B. Enns and J. K. Gillham, *J. Appl. Polymer Sci.*, **28,** 2567 (1983).
34. Y. C. Jean, *Microchem. J.*, **42,** 72 (1990).
35. R. A. Venditti, J. K. Gillham, Y. C. Jean, and Y. Lou, *J. Appl. Polym. Sci.*, **56,** 1207 (1995).
36. S. L. Simon and J. K. Gillham, *J. Appl. Polym. Sci.*, **47,** 461 (1993).
37. A. Hale, C. W. Macosko, and H. Bair, *Macromolecules,* **24,** 2610 (1991).
38. E. F. Oleinik in *Advances in Polymer Science 80, Epoxy Resins and Composites IV,* K. Dusek, Ed., Springer–Verlag, Berlin, 1986, pp. 49–99.
39. P. R. Couchman and F. E. Karasz, *Macromolecules,* **11,** 117 (1978).
40. P. R. Couchman, *Polym. Eng. Sci.*, **24,** 135 (1984).
41. R. A. Venditti and J. K. Gillham, *Proc. ACS: Polym. Mat.: Sci. Eng. Div.*, **69,** 434 (1993).
42. M. T. Aronhime and J. K. Gillham, *J. Coatings Technol.*, **56(718),** 35 (1984).

Received August 4, 1994
Accepted October 7, 1994